



Macro kinetic studies for photocatalytic degradation of benzoic acid in immobilized systems

Kanheya Mehrotra, Gregory S. Yablonsky¹, Ajay K. Ray^{*}

*Department of Chemical and Biomolecular Engineering, National University of Singapore,
10 Kent Ridge Crescent, Singapore 119260, Singapore*

Received 24 September 2004; received in revised form 18 January 2005; accepted 18 January 2005

Abstract

Semiconductor photocatalytic process has been studied extensively in recent years due to its intriguing advantages in environmental remediation. In this study, a two-phase swirl-flow monolithic-type reactor is used to study the kinetics of photocatalytic degradation of benzoic acid in immobilized systems. Transport contributions into the observed degradation rates were determined when catalyst is immobilized. Intrinsic kinetic rate constants and its dependence on light intensity and catalyst layer thickness, values of adsorption equilibrium constant, internal as well as external mass transfer parameters were determined. The simultaneous effect of catalyst loading and light intensity and optimum catalyst layer thickness were also determined experimentally. Reaction rate constants and overall observed degradation rates were compared with slurry systems.

© 2005 Published by Elsevier Ltd.

Keywords: Photocatalysis; Mass transfer; TiO₂; Optimum catalyst layer thickness; Intrinsic kinetic rate constant

1. Introduction

The photocatalytic oxidation of organic species dissolved in water is of great interest in recent years. This is evident from the numerous review papers that have been devoted to this field (Fox and Dulay, 1993; Mills et al., 1993; Hoffmann et al., 1995; Herrmann, 1999; Bahnemann, 2000). The process couples low energy ultraviolet light with semiconductors acting as photocatalysts. In this process, electron–hole pairs that are generated by the band-gap excitation carry out in situ

degradation of toxic pollutants. The holes act as powerful oxidant to oxidize toxic organic compounds while electrons can reduce toxic metal ions to metals, which can subsequently be recovered by solvent extraction (Chen and Ray, 2001). Photocatalytic degradation offers certain advantages over the traditional water treatment methods. Complete destruction of most contaminants is possible without the need of additional oxidizing chemicals such as hydrogen peroxide or ozone. Degussa P25 TiO₂ is widely used as the photocatalyst, which requires UV-A light ($\lambda < 380$ nm) of intensity 1–5 W m⁻² for photo excitation. The catalyst is cheap and can also be activated with sunlight (Chen et al., 2000a).

TiO₂ catalyst has been used in two forms: freely suspended in aqueous solution and immobilized onto rigid inert surface. In the former case, a high ratio of illuminated catalyst surface area to the effective reactor

^{*} Corresponding author. Tel.: +65 6874 8049; fax: +65 6779 1936/1937.

E-mail address: cheakr@nus.edu.sg (A.K. Ray).

¹ Present address: Department of Chemical Engineering, Washington University, St. Louis, MO, USA.

volume can be achieved for a small, well designed photocatalytic reactor (Ray and Beenackers, 1997), and almost no mass transfer limitation exists since the diffusional distance is very small, resulting from the use of ultrafine (<30 nm) catalyst particles (Chen and Ray, 1998). In large-scale applications, however, the catalyst particles must be filtered prior to the discharge of the treated water, even though TiO₂ is harmless to environment. Hence, a liquid–solid separator must follow the slurry reactor. The installation and operation of such a separator will raise the cost of the overall process, as the separation of the ultrafine catalyst particles is a slow and expensive process. Besides, the penetration depth of the UV light is limited due to the strong absorption by TiO₂ and dissolved organic species, particularly for dyes. All these disadvantages render the scale-up of a slurry reactor very difficult (Mukherjee and Ray, 1999).

The preceding problem can be eliminated by immobilizing TiO₂ catalyst over suitable supports (Matthews, 1987; Ray and Beenackers, 1998a,b). Design and development of immobilized thin catalyst film makes it possible for commercial-scale applications of TiO₂ based photocatalytic processes for water treatment (Ray, 1998, 1999; Sengupta et al., 2001). The designs are more likely to be useful in commercial applications as it provides at least three important advantages. Firstly, it eliminates the need for the separation of the catalyst particles from the treated liquid and enables the contaminated water to be treated continuously. Secondly, the catalyst film is porous, and can therefore provide a large surface area for the degradation of contaminant molecules. Thirdly, when a conductive material is used as support, the catalyst film can be connected to an external potential to remove excited electrons to reduce electron–hole recombination, thereby significantly improving the process efficiency (Hepel and Luo, 2001). However, Immobilization of TiO₂ on supports also creates its own problems (Periyathamby and Ray, 1999). There are at least two obvious problems arising from this arrangement: the accessibility of the catalytic surface to the photons and the reactants, and significant influence of external mass transfer particularly at low fluid flow rate, due to the increasing diffusional length of reactant from bulk solution to the catalyst surface. While on the other hand, with the increase of catalyst film thickness, the internal mass transfer may play a dominant role by limiting utilization of the catalyst near the support surface. All these usually lead to a lower overall degradation rate when catalyst is immobilized compared with the suspended system (Matthews, 1987). Surprisingly, there are very few investigations (Ray and Beenackers, 1997; Chen and Ray, 1999; Chen et al., 2000b), which offer a rational approach to study the influence of mass transfer in immobilized catalyst films, although studies in photocatalytic field have reached the pre-industry stage.

In this study, a novel semi-batch swirl-flow monolithic-type reactor is used to study the kinetics of photocatalytic reactions. Monoliths are unique catalyst supports that provide a high surface-to-volume ratio and allow high flow rates with low-pressure drop. The catalyst was immobilized for continuous use and to eliminate the need of separation for post-process treatment. Experiments are performed systematically to determine the various rate constants. The goals of this paper are to estimate transport contributions into the apparent kinetic rate parameters when catalyst is immobilized, calculation of the intrinsic kinetic parameters using the fixed catalyst data, and finally, to compare these parameters with corresponding values obtained from the slurry reactor. Values of adsorption equilibrium constant, internal as well as external mass transfer parameters were also evaluated. The simultaneous effect of catalyst loading and light intensity and optimum catalyst layer thickness were determined experimentally.

2. Experimental details

The semi-batch reactor consisted of two circular glass plates each of diameter 0.09 m that were placed between soft padding housed within stainless steel and aluminum casing separated by 0.01 m. The catalyst was deposited on the top of the bottom glass plate. The aqueous solution was introduced tangentially into the reactor by a peristaltic pump from a beaker with a water jacket, and exited from the center of the top plate as shown in Fig. 1. The exit tubing was also connected to that beaker. The tangential introduction of liquid created a swirl-flow and thereby minimizing mass transfer of pol-

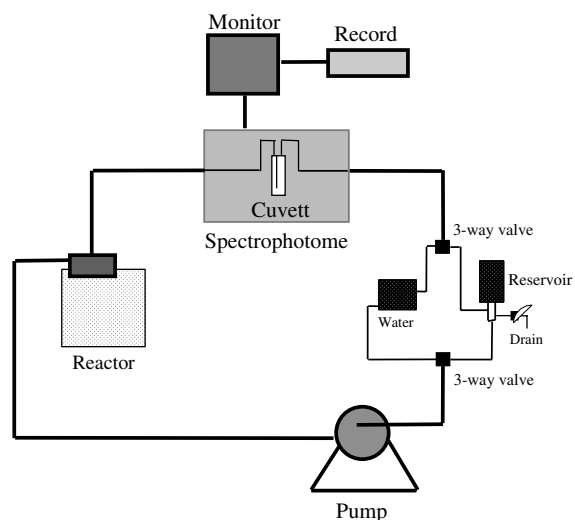


Fig. 1. Flow diagram of the experimental set-up.

lutants to the catalyst surface. The lamp (Philips HPR 125 W high pressure mercury vapor) was placed 0.1 m underneath the bottom glass plate on a holder that could be moved to create a different angle of incidence of light on the catalyst plate. The lamp and reactor were placed inside a wooden box painted black so that no stray light can enter into the reactor. The lamp was constantly cooled by a fan to keep the temperature down and protect the lamp from overheating. The lamp has a spectral energy distribution with a peak at $\lambda = 365.5$ nm of 2.1 W and thereby the incident light intensity was 213 W m^{-2} . Provision was made for placement of several metal screens of different mesh size between the lamp and bottom glass plate to obtain variation in light intensity. The light intensity was measured using a radiometer (UVP Model UVX-36).

Degussa P25 catalyst provided by Degussa Company (Germany) was used throughout this work without further modification. Its physico-chemical characteristics are as follows: BET surface area $55 \pm 15 \text{ m}^2 \text{ g}^{-1}$, average primary particle diameter is around 30 nm, purity above 98% and with anatase to rutile ratio as 80:20. Benzoic acid (99.5+%) was obtained from BDH Chemicals. All chemicals were used as received. Water used in this work was always Millipore water (from Milli Q plus185 ultra pure water system).

A Shimadzu 5000A TOC analyzer with an ASI-5000 auto-sampler was used to analyze the TOC in samples. Concentration of benzoic acid in the reaction samples was analyzed by a HPLC (Perkin Elmer LC240). Aliquots of 20 μl were injected onto a reverse-phase C-18 column (Chrompack), and eluted with the mixture of acetonitrile (60%) and ultrapure water (40%) at a total flow rate of 1.5 ml min^{-1} . Absorbance at 229 nm was used to measure the concentration of above compounds by a UV/VIS detector (Perkin Elmer 785A). All water samples were filtered by Millex-HA filter (Millipore, 0.45 μm) before analyses. The Cyberscan 2000 pH meter was used to measure the pH value of the solution.

2.1. Immobilization of catalyst

Pyrex (surface was roughened by sand blasting for improved catalyst fixation), was chosen as the support material since it is transparent to UV radiation down to wavelength of about 300 nm. Moreover, it would cut-off any light below 300 nm to avoid direct photolysis taking place. The glass surface was carefully degreased, cleaned with 5% HNO_3 solution overnight, washed with water and then dried at 393 K. A 10% aqueous suspension of the catalyst was prepared with water out of Millipore Milli-Q water purification system. The suspension was mixed in an ultrasonic cleaner (Branson 2200) bath for 30 min to obtain a milky suspension that remained stable for weeks. The substrate was then coated with catalyst by inserting into the suspension and pulling it out

slowly by Dip-coating technique (Ray and Beenackers, 1998a). The catalyst coating was dried at 393 K for 30 min and then calcined in a furnace (Heraeus UT 6060) in a vertical position by raising the temperature gradually at a rate of 0.15 K s^{-1} (to avoid cracking of the film) to a final firing temperature of 573 K and held there for 3 h. Then, the glass plate is cooled down to room temperature using the same ramping rate. It is necessary to heat and cool the glass plate gradually or the catalyst film may crack. The above procedures could be repeated few times depending on the desired catalyst loading (thickness). The calcination temperature has a significant effect on the catalyst activity, because it can affect the physical properties of the catalyst, such as porosity, surface area, crystal size, etc. Chen and Ray (1999) have reported that the optimal calcination temperature is about 573 K. Finally, the catalyst film was brushed carefully and flushed with Millipore water to remove the loosely bound catalyst. The total amount of catalyst deposited per unit area was determined by weighing the glass plate before and after the deposition. Depending on the number of dipping, the amount of catalyst obtained was between 0.0015 and 0.035 kg m^{-2} .

2.2. Experimental procedures

Before placing catalyst plate inside the reactor, the light intensity on the top of a bare glass plate was measured with the digital radiometer. At the start of every experiment the reactor was filled with Milli-Q water and rinsed for several times before zero-setting the analytical instrument. The reactor and connecting lines were then filled with the benzoic acid solution and it was ensured that no air bubbles remained in the system. The change in the concentration was continuously analyzed and recorded. Before turning on the light, it is necessary to circulate this solution for about 30 min to ensure that the adsorption equilibrium of the pollutant on TiO_2 surface and oxygen pre-saturation of the solution has reached. Oxygen was introduced into the solution continuously to keep the concentration of oxygen in excess than stoichiometric requirement throughout the reaction. The flow rate of oxygen was measured by a gas flow meter (Tokyo Keiso, Japan Model: P-200-UO). At the end of the experiment the entire system was rinsed with Milli-Q water, catalyst plate was removed, dried and weighed again to determine any loss of catalyst during experimentation.

3. Results and discussions

Before the start of the photocatalytic reactions, experiments were conducted to investigate whether there is any direct photolysis reaction. It was observed that no direct photolysis takes place for benzoic acid. When

experiments were conducted in presence of catalyst but in absence of light, a small decrease in concentration of benzoic acid was observed due to adsorption of model compound on to the catalyst surface, which reached an equilibrium value within 15 min. Hence, before turning the light on, it was always ensured that the adsorption equilibrium has reached. Therefore, degradation of benzoic acid in presence of light and catalyst observed is entirely due to photocatalysis.

3.1. Dark reaction: determination of adsorption equilibrium constant

Adsorption equilibrium constants were determined from both dark reaction and photocatalytic reaction. The small rapid decrease in benzoic acid concentration in the absence of light (dark reaction) when a fresh catalyst plate was used can be attributed to the adsorption of benzoic acid onto the catalyst. The concentration of benzoic acid adsorbed on the surface was calculated from the difference between the initial and equilibrium (no more decrease with time) concentrations. When the results are plotted (Fig. 2), it appeared to follow a Langmuir adsorption isotherm:

$$C_{\text{ads}} = \frac{NK C_{\text{eq}}}{1 + K C_{\text{eq}}} \quad (1)$$

where C_{ads} and C_{eq} are the concentration of benzoic acid adsorbed and the equilibrium concentration of benzoic acid used, respectively; N and K are the saturation and adsorption equilibrium value, respectively. When the data were fitted with Eq. (1) or by a straight line in

$[1/C_{\text{ads}}]$ against $[1/C_{\text{eq}}]$ plot, the value of K is found to be 10.1 mM^{-1} .

3.2. Rate expressions

Heterogeneous photocatalytic degradations often follow Langmuir–Hinshelwood kinetics. For our semi-batch system, the intrinsic reaction rate, r_{rxn} , could be defined as

$$r_{\text{rxn}} = \frac{V_{\text{L}}}{V_{\text{R}}} \left[-\frac{dC_{\text{b}}}{dt} \right] = \frac{k_{\text{r}} K C_{\text{s}}}{1 + K C_{\text{s}}} \quad (2)$$

where V_{L} and V_{R} are the total volume of liquid treated (m^3) and volume of reactor (m^3) respectively, dC_{b}/dt is the observed rate (mM s^{-1}), k_{r} and K are the reaction rate constant (mM s^{-1}) and adsorption–desorption equilibrium constant (mM^{-1}) respectively, and C_{s} is the concentration of the reactant at the catalyst surface (mM) in equilibrium with the actual surface concentration. It is to be noted that it is difficult to estimate for both slurry and immobilized catalyst systems the exact value for the active catalyst surface area participating in photocatalytic reactions. In case of slurry systems, it is impossible to quantify the active surface area due to unreliable knowledge of depth of light penetration, pattern of catalyst mixing, average catalyst particle size (and distribution) due to agglomeration, etc. (Mehrotra et al., 2003). It is also very difficult to determine the active surface area in fixed (immobilized) catalyst systems as the structure, morphology, porosity (inter-particle pore distributions) and catalyst layer thickness varies. It is, therefore, impractical to compare the rates based

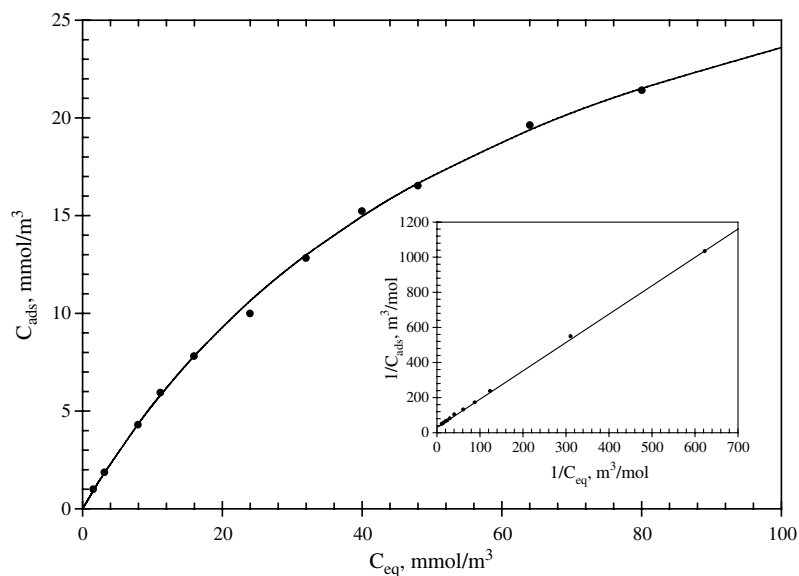


Fig. 2. Calculation of the adsorption equilibrium constant from dark reaction. Experimental condition: $Q = 5.83 \times 10^{-6} \text{ m}^3 \text{ s}^{-1}$, $V_{\text{L}} = 2.4 \times 10^{-4} \text{ m}^3$, $w = 0.0184 \text{ kg m}^{-2}$, $T = 303 \text{ K}$.

on active surface area for both the slurry and immobilized systems.

3.3. Determination of intrinsic reaction rate constant

Initial concentration of pollutant is always an important parameter in any process water treatment, and therefore, it is essential to examine the effect initial concentration. However, when the TiO_2 catalyst is coated on a support, it is expected that the mass transfer limitation would play a significant role in photocatalytic reactions due to the increased diffusional length for diffusion of contaminants from bulk solution to the catalyst surface. Therefore, in order to determine the intrinsic kinetic rates, it is necessary to eliminate the effect of mass transfer.

The kinetic expression in Eq. (2) is Langmuir type and it was found to be true when experiments were performed in slurry systems (Mehrotra et al., 2003). When catalyst is immobilized it would not be possible to determine the intrinsic kinetic parameters without knowing the concentration of the pollutant on the surface of the catalyst (C_s). However, when the initial concentration of the pollutant is high ($KC_s \gg 1$), the Langmuir type kinetic rate expression collapse to a zero-order rate expression and the overall rate would not depend on external mass transfer. Hence, if experiment is performed when catalyst film is thin (negligible internal mass transfer resistance) with high starting concentration of benzoic acid, and if concentration versus time plot shows a linear relationship, it would imply that the rate is zero-order. The $C-t$ plot in Fig. 3a shows linear relationship when experiments

were done at high initial concentration ($C_0 \approx 0.33$ mM). The constant degradation rate at two different circulation rate also suggests absence of external mass transfer. The true kinetic rate (k_r) can be determined from the slope of the concentration versus time plot and is obtained as $9.83 \times 10^{-5} \text{ mM s}^{-1}$. Recently, Mehrotra et al. (2003) reported photocatalytic degradation of benzoic acid in slurry systems in which they distinguished kinetic regime from transport (mass as well as light) limited regime and obtained intrinsic reaction rate constants for benzoic acid as $1 \times 10^{-4} \text{ mM s}^{-1}$. The true kinetic rate constants determined from fixed catalyst bed system is thus within 2% of the values obtained in the slurry system.

When the initial concentration of the pollutant is very low, ($KC_s \ll 1$), the kinetic rate expression given by Eq. (2) becomes a first-order rate expression. In this case, overall rate would certainly depend on mass transfer. For evaluation of true kinetic parameters it is necessary to eliminate mass transfer resistance. At steady-state the conversion rate follows

$$r_o = \left[\frac{V_L}{V_R} \right] \left[-\frac{dC_b}{dt} \right] = k_o C_b = k_{m,ext} \kappa (C_b - C_s) = \frac{k_r K C_s}{1 + K C_s} \quad (3)$$

where C_b and C_s are the concentration in the bulk and close to the catalyst surface, respectively in mol/m^3 , k_o (s^{-1}) is the first-order observed rate constant, $k_{m,ext}$ (m s^{-1}) is the external mass transfer rate and κ (m^{-1}) is the specific illuminated catalyst surface area ($\equiv A/V_R$). When $KC_s \ll 1$, Eq. (3) becomes

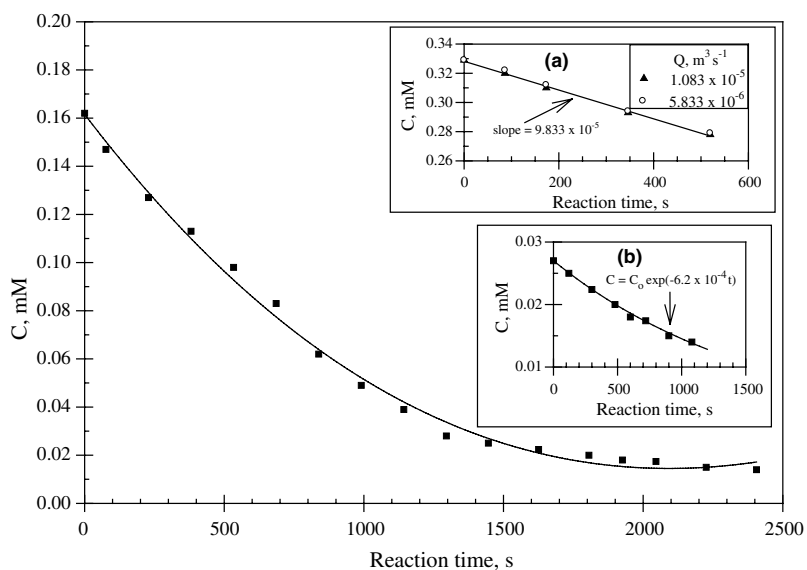


Fig. 3. Calculation of reaction rate constant of benzoic acid for fixed catalyst system. Experimental condition: $Q = 5.83 \times 10^{-6} \text{ m}^3 \text{ s}^{-1}$, $V_L = 2.4 \times 10^{-4} \text{ m}^3$, $w = 0.0184 \text{ kg m}^{-2}$, $I = 147 \text{ W m}^{-2}$, $T = 303 \text{ K}$, O_2 saturated, $\text{pH} = 3.7\text{--}3.9$.

$$r_o = k_{m,ext}\kappa(C_b - C_s) = k_r K C_s = k'_r C_s \quad (4)$$

where k'_r is the apparent first-order reaction rate constant (s^{-1}). From the above equation, we can solve for the unknown concentration C_s as

$$C_s = \left[\frac{k_{m,ext}\kappa}{k_{m,ext}\kappa + k'_r} \right] C_b \quad (5)$$

The above equation can be substituted in Eq. (4) to give

$$r_o = k_o C_b = \left[\frac{k'_r k_{m,ext}\kappa}{k_{m,ext}\kappa + k'_r} \right] C_b = \left[\frac{1}{\left[\frac{1}{k'_r} \right] + \left[\frac{1}{k_{m,ext}\kappa} \right]} \right] C_b \quad (6)$$

In other words, the various rates (observed, kinetic and mass transfer rate) are related, as

$$\frac{1}{k_o} = \frac{1}{k'_r} + \frac{1}{k_{m,ext}\kappa} = \frac{1}{k_r K} + \frac{1}{k_{m,ext}\kappa} \quad (7)$$

In addition to external mass transfer resistance, when catalyst is immobilized on a surface, internal mass transfer resistance might also exist, particularly for thick film. The internal mass transfer resistance results from the diffusion of organic molecules within the porous catalyst film. When catalyst is present as film, entire catalyst surface is not accessible to reactant, as reactant must diffuse through the layers of catalyst. In that case, the relationship among the observed degradation rate, the external and internal mass transfer rates and the intrinsic kinetic reaction rate are given by the following expression:

$$\frac{1}{k_o} = \frac{1}{k'_r} + \frac{1}{k_{m,int}\kappa} + \frac{1}{k_{m,ext}\kappa} \quad (8)$$

In order to determine intrinsic kinetic parameters it is necessary to find out the mass transfer rates, so that true kinetic parameters could be deduced from the overall observed rates.

3.4. Effect of internal mass transfer

The influence of the internal mass transfer on the observed photocatalytic reaction rate can be determined by the magnitude of the Thiele modulus. The thin catalyst film can be considered a porous slab and for the first order reaction, the Thiele modulus (Φ_H) is given by

$$\Phi_H = H \sqrt{\frac{k'_r}{D_e}} \quad (9)$$

where H is the thickness of the catalyst film, k'_r is the first-order kinetic rate constant, and D_e is the effective diffusivity of the pollutant within the catalyst film. Chen et al. (2000b) reported experimentally determined value of the effective diffusivity for benzoic acid as $1 \times 10^{-10} \text{ m}^2 \text{ s}^{-1}$. Using the rate constant (k_r) value obtained earlier as $9.83 \times 10^{-5} \text{ mM s}^{-1}$ and K from dark reaction as 10.1 mM^{-1} and film thickness in the range

of 2–5 μm , the Thiele modulus value is between 0.0063 and 0.0157, which is $\ll 1$. Therefore, internal mass transfer resistance could be neglected as in our study most of the experiments were conducted at low catalyst loading of 0.02 kg m^{-2} . It is worth noting that the internal mass transfer is an intrinsic property of the catalyst film, which depends on the nature of the catalyst, coating techniques, pre-and post treatment of catalyst films, etc.

3.5. Effect of external mass transfer

If the external mass transfer resistance exists, the reaction rate will depend on the circulation flow rate (Q), particularly when circulation flow rate is low. The external mass transfer resistance can be reduced to a minimum by increasing mixing of fluid through stirring or increasing the circulating flow rate (Reynolds number, Re) of the reaction medium. Experimental results for the effect of circulation flow rates on photocatalytic degradation benzoic acid are shown in Fig. 4. The figure confirms significant external mass transfer limitation when catalyst is fixed (immobilized) on a surface.

3.6. Determination of the external mass transfer rate

In this study, the external mass transfer coefficient, $k_{m,ext}$, was determined experimentally by measuring the dissolution rate of benzoic acid into water ($C_{out}/C_{sat} \approx 0.04$) at different flow rates at 303 K. The benzoic acid was coated on the inside of the bottom glass plate. The process could be described by the following equation:

$$V_L \frac{dC_b}{dt} = -k_{m,ext} A (C_b - C_s) \quad (10)$$

where V_L is the total liquid volume (m^3), A is the available surface area of benzoic acid film (m^2), C_s and C_b are the concentration of benzoic acid on the surface of the film and in the bulk solution (mM), respectively. As benzoic acid is sparingly soluble in water, C_s was assumed to be equal to the solubility of benzoic acid in water. The experimental results are shown in Fig. 5 as a function of the Reynolds number (Re), together with the best fit:

$$k_{m,ext} \text{ (in } \text{m s}^{-1}\text{)} = 9.5 \times 10^{-7} Re^{0.77} \quad (11)$$

It is worth noting that at high circulation flow rate external mass transfer resistance will be minimum. However, physical limitation on the equipment prevents us from using very high circulation flow rate, since at very high flow rate bubbles will be introduced inside the reactor, which will lead to the significant experimental error during measurement. Considering the above fact, all subsequent experiments were performed at a circulation flow rate of $5.83 \times 10^{-6} \text{ m}^3 \text{ s}^{-1}$, which is equivalent to Reynolds number of 106.

The intrinsic rate constants k_r obtained from Fig. 3a (when experiments were conducted at high initial concen-

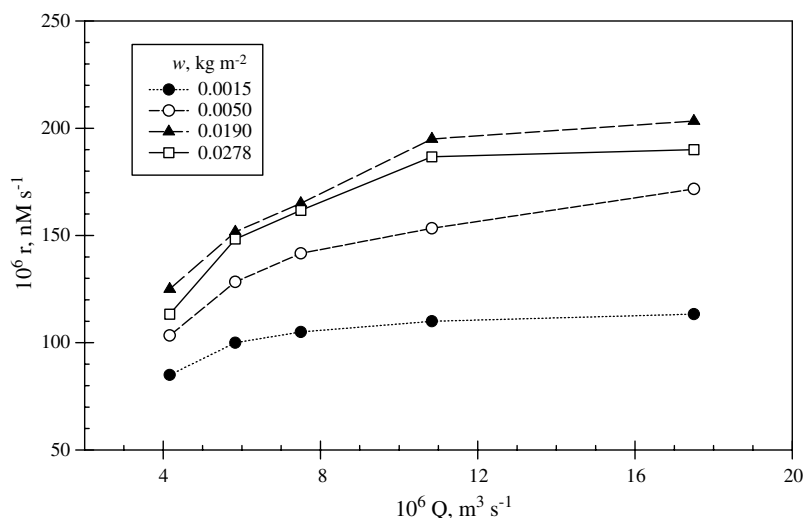


Fig. 4. Effect of circulation rate on the photocatalytic degradation of benzoic acid for various catalysts loading. Experimental condition: $C_0 = 0.16 \text{ mol/m}^3$, $V_L = 2.4 \times 10^{-4} \text{ m}^3$, $I = 147 \text{ W m}^{-2}$, $T = 303 \text{ K}$, O_2 saturated, $\text{pH} = 3.7\text{--}3.9$.

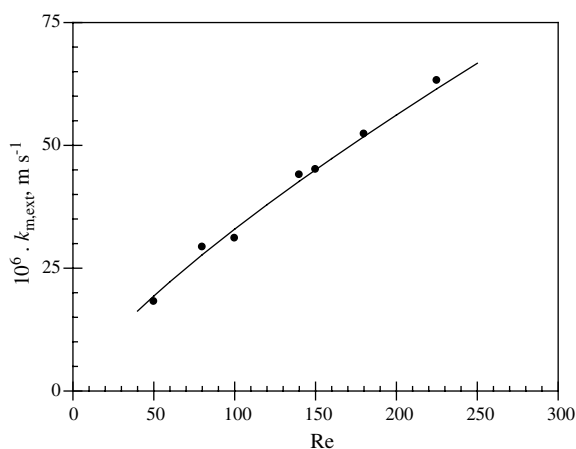


Fig. 5. Calculation of external mass transfer coefficient, $k_{m,\text{ext}}$, as function of Reynolds number, Re . Experimental condition: $V_L = 2.4 \times 10^{-4} \text{ m}^3$, $T = 303 \text{ K}$, $A = 0.0038 \text{ m}^2$.

tration) is $9.83 \times 10^{-5} \text{ mM s}^{-1}$, and the observed first-order rate constant, $k'_r (\equiv k_r K)$, obtained from Fig. 3b (when experiments were conducted at low initial concentration) is $6.2 \times 10^{-4} \text{ s}^{-1}$. Using the value of $k_{m,\text{ext}}$ from Eq. (11) for $Re = 106$ and $\kappa (\equiv A/V_R)$ as 59.7 m^{-1} , the value of K from Eq. (7) can be determined as 9.925 mM^{-1} , which is within 2% of the value obtained from the dark reaction experiments (Fig. 2), thus suggesting that K indeed represents adsorption characteristics.

3.7. Effect of light intensity

It is obvious that light intensity has great effect on photocatalytic reaction rate. The reaction rate constant

usually follows power-law dependence on light intensities. In order to investigate the relationship between the reaction rate constant, k_r , and light intensity, I , experiments were conducted at varying light intensity on a thin layer of catalyst film in order to minimize internal mass transfer resistance. The intensity of light falling on the catalyst was varied in our experimental set-up by placing different mesh size screens between the lamp and the bottom glass plate. At low concentration of benzoic acid, it was found that the observed rate follows first-order dependence. The true first-order rate constants (k_r) calculated after correcting for external mass transfer (using k_m as discussed before) are plotted for different values of light intensity in Fig. 6. When the data of k_r (expressed as s^{-1}) and I (expressed as W m^{-2}) was fitted with an empirical power law equation

$$k_r = aI^\beta \quad (12)$$

we found the values of a and β as 8.82×10^{-6} and 0.89 respectively.

3.8. Combined effect of catalyst loading and light intensity on the degradation rate

The catalyst layer thickness (amount of catalyst) is an important parameter in photocatalytic degradation. As in aqueous suspension (Mehrotra et al., 2003), there also exists an optimal catalyst dosage for fixed catalyst system. In the slurry system, this is due to the increase of internal (inter-particle agglomeration) mass transfer resistance and light shielding effect, which will result in the decrease of overall reaction rate with the increase of catalyst loading (Mehrotra et al., 2003). Ray and Beenackers (1997) were the first to report some studies on

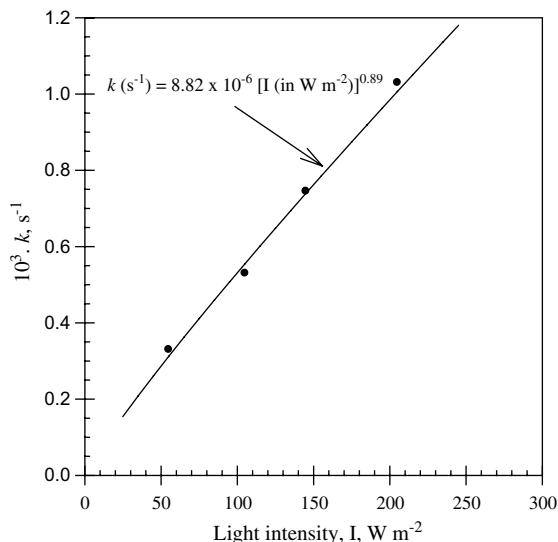


Fig. 6. Effect of light intensity on the reaction rate constant of benzoic acid. Experimental condition: $C_0 = 0.16$ mM, $V_L = 2.4 \times 10^{-4}$ m³, $Re = 106$, $w = 0.0184$ kg m⁻², $T = 303$ K, O₂ saturated, pH = 3.7–3.9.

the effect of catalyst layer thickness for fixed catalyst system on the photocatalytic degradation of SBB textile dye. Subsequently, Chen et al. (2000b) reported detailed analysis of the effect of mass transfer and catalyst layer thickness on photocatalytic degradation rate. In this work, experiments were performed for photocatalytic degradation of benzoic acid using different catalyst load-

ing and light intensity and the results are shown in Fig. 7. Experimental result shows that photocatalytic rate goes through a maximum at an optimum catalyst loading (0.0184 kg m⁻²) irrespective of incident light intensity. In fixed catalyst system, the pollutant (benzoic acid) diffuses from the bulk solution through a boundary layer (liquid-film mass transfer resistance) to reach the liquid-catalyst interface. Subsequently, the reactant diffuses through the catalyst layers (inter-particle diffusion) to locate active sites where they get adsorbed and react. At the same time, UV light must also reach the catalyst surface to activate the catalyst. It is worth noting that there is no boundary resistance for UV light penetration (transmission) and Degussa P25 TiO₂ is a nonporous catalyst, thus there is no intra-particle diffusion.

There are two counteracting affects, which is resulting this optimum rate. The increase of the catalyst loading increases the degradation rate due to more available catalyst surface sites but at the same time there are two likely loss mechanisms within the catalyst films due to increase of the catalyst layer thickness that will restrict the presence of charge carriers at the interface. One is attenuation of light due to absorption by the catalyst, and the other is the increased probability of charge carrier recombination presumably due to the increased diffusional lengths through the grain boundaries and constrictions within the micro-porous film. Within the bulk of the catalyst film, the extinction of light follows the exponential decay (Chen et al., 2000b). Fig. 8 indicates that the photocatalytic rate reaches a saturation value as the catalyst layer thickness increases. This can be understood

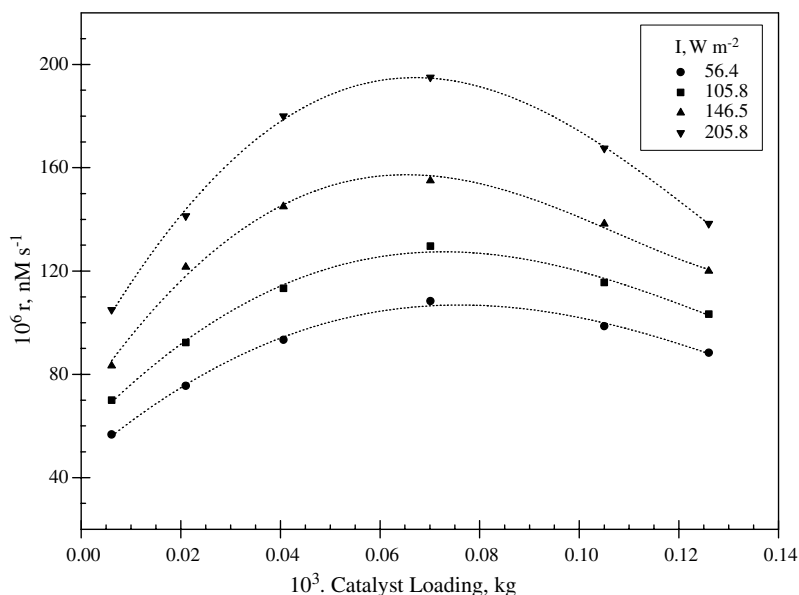


Fig. 7. Effect of catalyst loading and light intensity on the photocatalytic degradation of benzoic acid. Experimental condition: $C_0 = 0.16$ mM, $V_L = 2.4 \times 10^{-4}$ m³, $Re = 106$, $T = 303$ K, O₂ saturated, pH = 3.7–3.9.

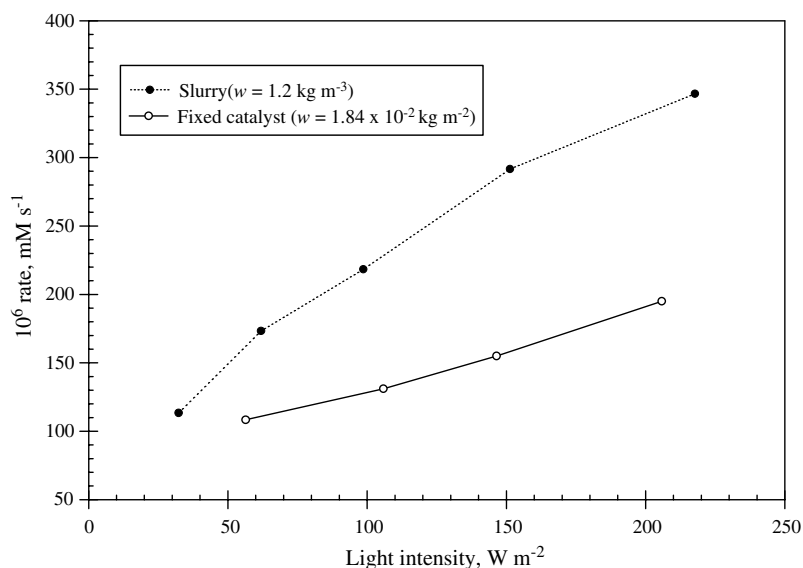


Fig. 8. Comparison of photocatalytic degradation rate of benzoic acid between slurry and fixed catalyst system at optimum catalyst loading. Experimental condition: $C_0 = 0.16$ mM, $V_L = 2.4 \times 10^{-4}$ m³, $Re = 106$, $T = 303$ K, O₂ saturated, pH = 3.7–3.9, $w = 1.2$ kg m⁻³ (slurry), 0.0184 kg m⁻² (fixed).

if we look at the physical problem. When the catalyst film is thin, the absorption of light will not be strong enough as wavelength of light ($\lambda = 0.365$ μm) is of the same order of magnitude that of the film thickness, and consequently, the catalyst layer will not be active to its highest possible level. As the film thickness increases, at some point the penetration depth of light will be such that most of the electrons and holes are generated relatively close to the solid–liquid interface. The photocatalytic reaction rate will be about maximum at this point. With further increase in the film thickness (thicker film), the charge carriers generated relatively far from the liquid–catalyst interface, and consequently, are more susceptible to recombination loss. A further increase of film thickness will lower the photocatalytic reaction rate.

3.9. Estimation of internal mass transfer coefficient, $k_{m,int}$

When the amount of catalyst loading is increased the internal mass transfer resistance increases as the film thickness increases. Fig. 8 showed that the photocatalytic reaction rate attains a maximum at an optimum catalyst layer thickness, H_{opt} . Chen et al. (2000b) derived an expression of the optimum catalyst layer thickness as

$$H_{opt} = \frac{\ln \left[\frac{\alpha \beta D_e}{k_{m,int}} \right]}{\left[\alpha \beta - \frac{k_{m,int}}{D_e} \right]} \quad (13)$$

where α is the light absorption coefficient factor determined experimentally by Chen et al. (2000b) as

$0.6264 \mu\text{m}^{-1}$, β is kinetic factor defined in Eq. (12) and obtained as 0.89 in this study, D_e is the effective diffusivity of benzoic acid within the catalyst film and obtained experimentally as 1×10^{-10} m² s⁻¹ (Chen et al., 2000b), and $k_{m,int}$ is the internal mass transfer coefficient. The optimum catalyst layer thickness can be correlated as

$$H_{opt} = \frac{W_{opt}}{A \rho_{cat}} \quad (14)$$

where W_{opt} is the total amount of catalyst (kg), A is the surface area of the catalyst coated plate (m²), and ρ_{cat} is the density of the catalyst (kg m⁻³). In our study, $W_{opt} = 7 \times 10^{-5}$ kg (see Fig. 7), $A = 0.0038$ m², and $\rho_{cat} = 3.8 \times 10^3$ kg m⁻³, which results in $H_{opt} = 4.85$ μm . Using the values of H_{opt} , α , β and D_e mentioned above, the value of $k_{m,int}$ is obtained as 4.75×10^{-6} m s⁻¹. Hence, at the optimum catalyst layer thickness, the internal mass transfer resistance is comparable to the external mass transfer resistance.

3.10. Comparison of slurry system with fixed catalyst system

Mehrotra et al. (2003) carried out systematic analysis to distinguish kinetic and transport limited regimes for photocatalytic degradation of benzoic acid in slurry systems. They reported optimum catalyst loading of 1.2 kg m⁻³ for slurry systems. Fig. 8 compares the rate of degradation of benzoic acid between slurry system (at optimum catalyst loading of 1.2 kg m⁻³) and fixed catalyst system (at optimum catalyst loading of 0.0184

kg m⁻²) at different light intensities. It is expected that the degradation rate for the slurry system is higher than fixed catalyst system and in our study we found that rates for slurry system is about 40% higher than fixed catalyst system. However, it should be noted that it is convenient to scale-up fixed catalyst system compared to slurry system for photocatalytic degradation and moreover, it will circumvent the problem of separation of ultrafine catalyst particles after treatment.

4. Conclusions

A swirl-flow, monolithic-type reactor was used to evaluate the intrinsic kinetic parameters for photocatalytic degradation of benzoic acid when Degussa P25 TiO₂ catalyst was immobilized on the Pyrex glass substrate by dip-coating technique. The reactor is unique for kinetic study of photocatalysis, as it can be used to measure, apart from various rate constants, the effects of the catalyst layer thickness and light intensity on the rate constants. It was found that external mass transfer resistance exists, and true kinetic rates were calculated from the observed reaction rate after correcting for mass transfer resistance. Optimum catalyst layer thickness, internal mass transfer coefficient, and dependence of light intensity on reaction rates were determined experimentally. The rate constants and overall rates were compared to slurry system and it was found that at optimum conditions the observed rate of degradation is 40% more than fixed catalysts systems.

References

- Bahnemann, D.W., 2000. Current challenges in photocatalysis: Improved photocatalysts and appropriate photoreactor engineering. *Res. Chem. Intermediat.* 26, 207–220.
- Chen, D.W., Ray, A.K., 1998. Photodegradation kinetics of 4-nitrophenol in TiO₂ aqueous suspensions. *Water Res.* 32, 3223–3234.
- Chen, D.W., Ray, A.K., 1999. Photocatalytic kinetics of phenol and its derivatives over UV irradiated TiO₂. *Appl. Catal. B: Environ.* 23, 143–157.
- Chen, D.W., Ray, A.K., 2001. Removal of toxic metal ions in wastewater by semiconductor photocatalysis. *Chem. Eng. Sci.* 56, 1561–1570.
- Chen, D.W., Sivakumar, M., Ray, A.K., 2000a. Semiconductor photocatalysis in environmental remediation. *Dev. Chem. Eng. Mineral Process.* 8, 505–550.
- Chen, D.W., Li, F.M., Ray, A.K., 2000b. Effect of mass transfer and catalyst layer thickness on photocatalytic reaction. *AIChE J.* 46, 1034–1045.
- Fox, M.A., Dulay, M.T., 1993. Heterogeneous photocatalysis. *Chem. Rev.* 93, 341–357.
- Hepel, M., Luo, J., 2001. Photoelectrochemical mineralization of textile diazo dye pollutants using nanocrystalline WO₃ electrodes. *Electrochim. Acta* 47, 729–740.
- Herrmann, J.M., 1999. Heterogeneous photocatalysis: fundamentals and applications to the removal of various types of aqueous pollutants. *Catal. Today* 53, 115–129.
- Hoffmann, M.R., Martin, S.T., Choi, W.Y., Bahnemann, D.W., 1995. Environmental applications of semiconductor photocatalysis. *Chem. Rev.* 95, 69–96.
- Matthews, R.W., 1987. Photooxidation of organic impurities in water using thin films of titanium dioxide. *J. Phys. Chem.* 91, 3328–3333.
- Mehrotra, K., Yablonsky, G.S., Ray, A.K., 2003. Kinetic studies of photocatalytic degradation in TiO₂ slurry system: distinguishing working regimes and determining rate dependences. *Ind. Eng. Chem. Res.* 42, 2273–2281.
- Mills, A., Davies, R.H., Worsley, D., 1993. Water purification by semiconductor photocatalysis. *Chem. Soc. Rev.* 22, 417–425.
- Mukherjee, P.S., Ray, A.K., 1999. Major challenges in the design of a large-scale photocatalytic reactor for water treatment. *Chem. Eng. Technol.* 22, 253–260.
- Periyathamby, U., Ray, A.K., 1999. Computer simulation of a novel photocatalytic reactor using distributive computing environment. *Chem. Eng. Technol.* 22, 881–888.
- Ray, A.K., 1998. A new photocatalytic reactor for destruction of toxic water pollutants by advanced oxidation process. *Catal. Today* 44, 357–368.
- Ray, A.K., 1999. Design, modeling, and experimentation of a new large-scale photocatalytic reactor for water treatment. *Chem. Eng. Sci.* 54, 3113–3125.
- Ray, A.K., Beenackers, A.A.C.M., 1997. Novel swirl-flow reactor for kinetic studies of semiconductor photocatalysis. *AIChE J.* 43, 2571–2578.
- Ray, A.K., Beenackers, A.A.C.M., 1998a. Novel photocatalytic reactor for water purification. *AIChE J.* 44, 477–483.
- Ray, A.K., Beenackers, A.A.C.M., 1998b. Development of a new photocatalytic reactor for water purification. *Catal. Today* 40, 73–83.
- Sengupta, T.K., Kabir, M.F., Ray, A.K., 2001. A Taylor vortex photocatalytic reactor for water purification. *Ind. Eng. Chem. Res.* 40, 5268–5281.